

## Effect of temperature and time on solvothermal synthesis of tetragonal BaTiO<sub>3</sub>

AMIR HABIB<sup>1,2,\*</sup>, NILS STELZER<sup>2</sup>, PAUL ANGERER<sup>3</sup> and ROLAND HAUBNER<sup>4</sup>

<sup>1</sup>School of Chemical and Materials Engineering, National University of Science and Technology, H/12 Islamabad, Pakistan

<sup>2</sup>Austrian Institute of Technology GmbH, Advanced Materials & Aerospace Technologies, A-2444 Seibersdorf, Austria

<sup>3</sup>Centre of Electrochemical Surface Technology, A-2700 Wiener Neustadt, Austria

<sup>4</sup>Vienna University of Technology, Getreidemarkt 9/164-CT, A-1060 Vienna, Austria

MS received 29 July 2009; revised 16 October 2009

**Abstract.** Tetragonal BaTiO<sub>3</sub> nanoparticles are synthesized via solvothermal route in an ethanol water mixture. Ba(OH)<sub>2</sub>·8H<sub>2</sub>O is used as Ba precursor and TiO<sub>2</sub> (P25 Degussa ~25 nm, 30% anatase, 70% rutile) is used as Ti precursor in the Ba : Ti molar ratio 2 : 1. Effect of temperature and time study on solvothermal synthesis of BaTiO<sub>3</sub> revealed that a moderate reaction temperature i.e. 185°C and longer reaction time favour tetragonal phase stabilization. Dissolution–precipitation appears to be the transformation mechanism for the crystallization of BaTiO<sub>3</sub> from particulate TiO<sub>2</sub> precursor.

**Keywords.** Powders—chemical preparation; X-ray methods; electron microscopy; BaTiO<sub>3</sub>; tetragonal phase.

### 1. Introduction

A prime objective in the barium titanate synthesis is to create smaller, more uniform particles without the loss of dielectric properties via low-temperature synthesis mechanisms. Such finer particles with high relative permittivity may be used in multilayers ceramic capacitors to achieve device miniaturization (Yoon 2006) or embedded in the polymers to achieve thin dielectric layers (Habib *et al* 2009). Controlling the phase, composition homogeneity, particle size and monodispersity, microstructure, and the cost of particle production are other concerns in developing techniques for synthesizing barium titanate. The stable crystalline polymorph of BaTiO<sub>3</sub> at room temperature is the tetragonal form, which possesses a high dielectric constant at temperatures between 0°C and 130°C. Above 130°C the unit cell converts to a paraelectric cubic structure (Hench and West 1990). Among various methods for producing sub-micrometer BaTiO<sub>3</sub> powder, the hydrothermal technique is well known, however, in all the synthesis reactions below 250°C, the metastable cubic BaTiO<sub>3</sub> stabilizes (Kiss *et al* 1966; Vivekanandan *et al* 1987; Habib *et al* 2008). Hydrothermal synthesis of BaTiO<sub>3</sub> resulting in the stabilization of tetragonal form at room temperature has only been reported for syntheses that are carried out above 450°C (Christensen 1970; Kajiyoshi *et al* 1991). Recently, a few authors (Xu and Gao 2003; Kwon *et al* 2006; Sun *et al* 2006) have reported the synthesis of tetragonal

BaTiO<sub>3</sub> in nanometer size in the temperature range 210–240°C. Development of strains within the particles in the presence of OH<sup>−</sup> impurities at lattice sites prevents BaTiO<sub>3</sub> from assuming tetragonal phase (Dutta *et al* 1994). Therefore, a low temperature synthesis procedure that directly results in the formation of tetragonal BaTiO<sub>3</sub> is of interest. The present work aims at achieving the tetragonal BaTiO<sub>3</sub> in nanometer regime using ethanol–water mixture in 1:1 ratio as reaction medium below 200°C using Ba(OH)<sub>2</sub>·8H<sub>2</sub>O and TiO<sub>2</sub> (P 25 Degussa ~25 nm, 30% anatase, 70% rutile).

### 2. Experimental

The Ba to Ti ratio is kept at 2 : 1 in all experiments. Both precursors were weighed and added to a teflon vessel along with distilled water and ethanol in equal amounts i.e. 30 ml each. No mineralizer was used to adjust pH of the solution. The mixed Ba and Ti precursors were treated at different temperatures, 165, 185 and 235°C, for different reaction times in an autoclave (BLH800, Berghof, Germany) under autogenous pressure. All reactions took place at set times after the temperatures had reached a desired value. The obtained slurry was washed with 100 ml of 1 M formic acid and then dried in an oven at 100°C. The resulting dry cake was ground using an agate mortar to obtain BaTiO<sub>3</sub> powders.

The phase analysis of the samples was carried out by means of powder XRD methods (Young 1993; Dinnebieer and Billinge 2008). For this purpose an X'Pert device (Bragg–Brentano diffraction geometry, manufactured by Philips

\*Author for correspondence (habib\_amir@hotmail.com)

Panalytical, the Netherlands) was used. This apparatus uses  $\text{CuK}\alpha$  radiation (0.15406 nm wavelength) and is equipped with an automatic divergence slit, a graphite monochromator, and a scintillation counter. The measurements were conducted in step-scan mode in the range of  $5\text{--}85^\circ 2\theta$  with a step size of  $0.025^\circ$ . The XRD data evaluation (lattice parameters, crystallite size) was performed using the Rietveld analysis software package TOPAS by Bruker AXS, Germany (AXS 2005). A high resolution scanning electron microscopy — HRSEM ZEISS — Gemini Supra VP was used to investigate the particle size and morphology of the sample powders.

### 3. Results and discussion

The various samples obtained during solvothermal synthesis are shown in table 1. All the samples were obtained using Ba : Ti ratio = 2 : 1 in ethanol to water mixture (1 : 1).

#### 3.1 Crystal structure and phase

Figure 1(a) shows the X-ray diffraction patterns of obtained samples of  $\text{BaTiO}_3$  powders. The perovskite structure is evident in all the samples. No impurities like  $\text{BaCO}_3$  or  $\text{TiO}_2$  are observed in the samples indicating the crystallization of pure  $\text{BaTiO}_3$ . XRD patterns of obtained  $\text{BaTiO}_3$  for samples reacted at  $185^\circ\text{C}$  for 6 days shows a clear split of (002) and (200) peaks at  $44.85^\circ 2\theta$  and  $45.38^\circ 2\theta$ . This split decreases for shorter duration of reactions whereas at  $165^\circ\text{C}$  after 4 days the split becomes minimal.

#### 3.2 Tetragonality $c/a$

The ‘a’ and ‘c’ cell parameters were calculated using Rietveld analysis. The tetragonality is calculated in terms of  $c/a$  ratio for sample powders as shown in table 1. The highest value of  $c/a = 1.00828$  is obtained for samples synthesized by solvothermal processing at  $185^\circ\text{C}$  for 6 days.

The lowest value of  $c/a = 1.00611$  is observed for samples reacted at  $165^\circ\text{C}$  for 4 days. The samples obtained at  $185^\circ\text{C}$  after 3 days, at  $235^\circ\text{C}$  for 1 day and  $185^\circ\text{C}$  after 2 days have values close to each other. An increase in the value of  $c/a$ ,

**Table 1.** Crystallite size using XRD data and particle size from SEM images with different tetragonality ( $c/a$ ) ratios for obtained  $\text{BaTiO}_3$  powders.

Sample	Temperature (°C)	Time (days)	Crystallite size XRD (nm)	Particle size SEM (nm)	$c/a$
EtOH-1	185	6	66	120	1.008
EtOH-2	185	3	64	90	1.007
EtOH-3	185	2	48	–	1.007
EtOH-4	235	1	47	100	1.007
EtOH-5	165	4	57	90	1.006

with increase in reaction time i.e. 2, 3, and 6 days, is observed for samples reacted at  $185^\circ\text{C}$ .

#### 3.3 Crystallite size

Table 1 shows that the crystallite size obtained by the Rietveld calculations of the prepared powders remained between 47 and 66 nm. For powders obtained at  $185^\circ\text{C}$ , an increase in  $c/a$  with an increase in crystallite size is observed. The crystallite size of the sample obtained at  $185^\circ\text{C}$  after 6 days is 66 nm. The crystallite size for the sample obtained at  $165^\circ\text{C}$  after 4 days is 57 nm.

#### 3.4 Particle size and morphology

Figure 2 shows scanning electron micrographs of the obtained  $\text{BaTiO}_3$  powders. For all the samples, the homogeneous size distribution remains to be a typical characteristic of powders obtained via this solvothermal route.

The particle size appears to increase with reaction time. The particle size for samples obtained at  $185^\circ\text{C}$  after 6 days is around 120 nm, whereas its value is around 80–90 nm at same temperature after 3 days.

No trend of particle size variation is predictable on the basis of reaction temperatures (figure 3).

The morphology of obtained powders remains rectangular for a reaction temperature of  $185^\circ\text{C}$ . The samples obtained at  $235^\circ\text{C}$  after 1 day as well shows the rectangular shape of nanoparticles, whereas spherical particles are observed for a reaction temperature of  $165^\circ\text{C}$ .

The combined effect of solvent, temperature, pressure and time on the ionic reaction equilibrium stabilizes desirable single or multiple complex oxides during a hydrothermal/solvothermal process. The effect of synthesis conditions i.e. reaction temperature, and time on the formation of tetragonal phase of  $\text{BaTiO}_3$  observed in this work is supported by literature and is discussed here.

#### 3.5 Crystal structure and phase

No unreacted  $\text{TiO}_2$  is observed in the samples indicating the crystallization of pure perovskite  $\text{BaTiO}_3$ . Use of  $\text{Ba/Ti} > 1$  is beneficial for achieving phase pure  $\text{BaTiO}_3$  (Habib et al 2008). The splitting of the (200) reflection with the lower angle shoulder indexed at (002) is an indication of tetragonal form of  $\text{BaTiO}_3$  (Dutta et al 1994; Wu et al 1996; Lu et al 2000). In the cubic form this peak remains unsplit. The double peak is obvious in all the samples with varying amounts of tetragonality. Figure 1(b) shows these splitting peaks clearly, whereas figure 3(a) shows the corresponding variation of  $c/a$  ratios. This indicates that stabilization of tetragonal phase of  $\text{BaTiO}_3$  is dependent on reaction temperature and time. The  $c/a$  value and amount of splitting is observed to increase for a reaction temperature ( $185^\circ\text{C}$ ) as

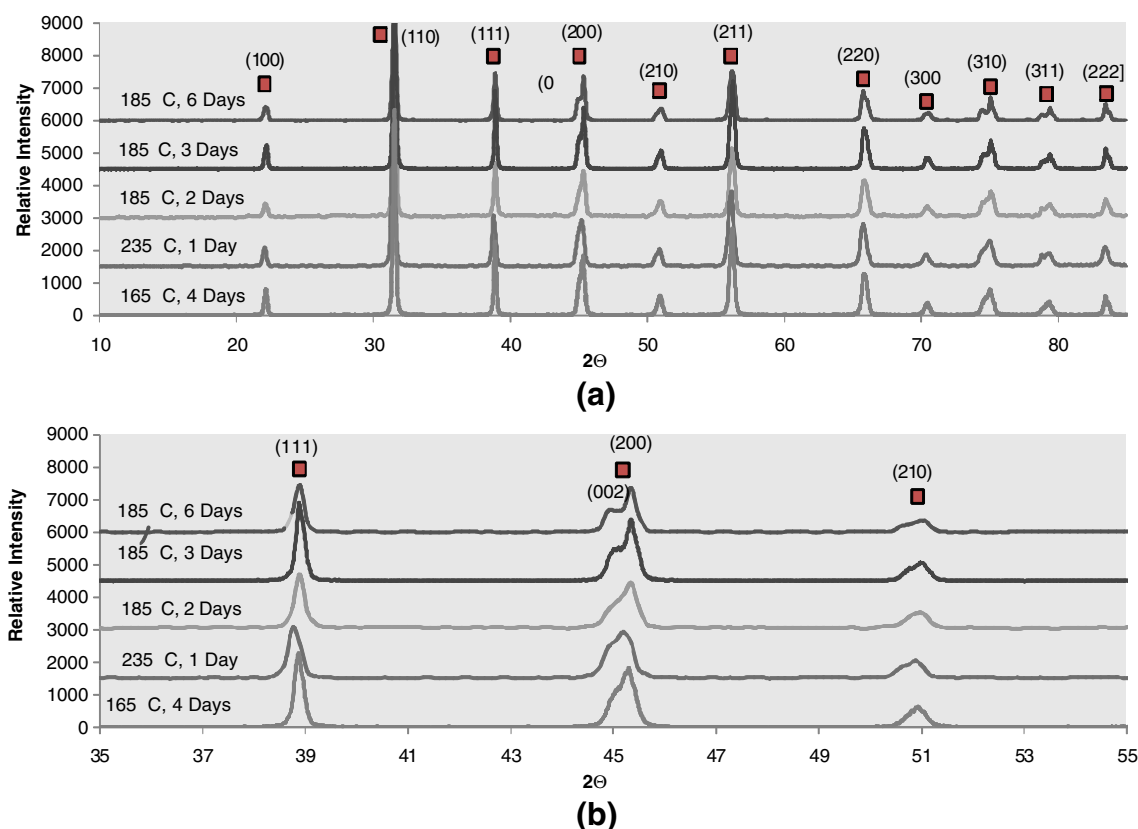


**Figure 1.** (a) XRD patterns of obtained BaTiO<sub>3</sub> samples, (b) enlarged portion of the graph to indicate the clear split in (002) and (200) peaks around 45° 2 $\theta$  angles.

the reaction time increases. Product at low reaction temperature i.e. 165°C, for four days has minimum  $c/a$  and split, whereas the reaction at 235°C for 1 day has as well yielded low tetragonality powder. This hints towards the slow crystallization kinetic of tetragonal BaTiO<sub>3</sub>. The same was found by Dutta and Gregg (1992) and Wu *et al* (1999), who reported hydrothermal synthesis of tetragonal BaTiO<sub>3</sub> after several days of reaction time.

### 3.6 Influence of ethanol during synthesis of BaTiO<sub>3</sub> powders

Presence of ethanol is another important factor that helps to form tetragonal phase of BaTiO<sub>3</sub> as reported by Kwon *et al* (2006). In a way our results enforce the idea of Kwon *et al* (2006) that OH<sup>-</sup> plays a vital role in stabilization of tetragonal phase. It is, however, difficult to say how OH<sup>-</sup> contributes to it, as the reaction in nonaqueous solution is complex and there is currently limited information available regarding kinetics and underlying crystallization mechanism. Two proposed mechanisms of formation of BaTiO<sub>3</sub> from Ba<sup>2+</sup> and Ti species involve a condensation reaction of Ti(OH)<sub>6</sub><sup>2-</sup> with Ba<sup>2+</sup> (Vivekanandan *et al* 1987) and migration of Ba<sup>2+</sup> into the TiO<sub>2</sub> structure with resulting breakage of Ti–O–Ti bonds and incorporation of Ba<sup>2+</sup> (Kiss *et al* 1966; Dutta and Gregg

1992). In the latter mechanism, the role of OH<sup>-</sup> ions could be to facilitate the hydrolysis of Ti–O–Ti bonds.

Chen and Jiao (2000) found the formation of BaTiO<sub>3</sub> difficult in solvothermal synthesis than in hydrothermal method. They reported the synthesis of cubic BaTiO<sub>3</sub> powders of <60 nm using ethanol and attributed loss of tetragonality to low permittivity of the solvent. However, this study, supported by Kwon *et al* (2006), shows that the ethanol itself is not detrimental, rather it is effective for tetragonal BaTiO<sub>3</sub> synthesis.

### 3.7 Tetragonality ratio and particle size effect

Begg *et al* (1994) reported that the largest  $c/a$  ratio was 1.010 for hydrothermally synthesized BaTiO<sub>3</sub> powders. Earlier literature (Buessem *et al* 1966; Bell *et al* 1984; Arlt *et al* 1985; Arlt 1987; Kanata *et al* 1987; Dutta and Gregg 1992) reported that to stabilize tetragonal BaTiO<sub>3</sub>, it is important that crystal size should exceed 1  $\mu$ m to accommodate the strains caused by the transformation from cubic to tetragonal structure. Few successful cases of tetragonal BaTiO<sub>3</sub> powder synthesis below 100 nm size have been reported recently (Lu *et al* 2000; Zhang *et al* 2001; Xu and Gao 2003; Kwon *et al* 2006). This study reports the synthesis of BaTiO<sub>3</sub> powders at 185°C with crystallite size, 66 nm and high tetragonality

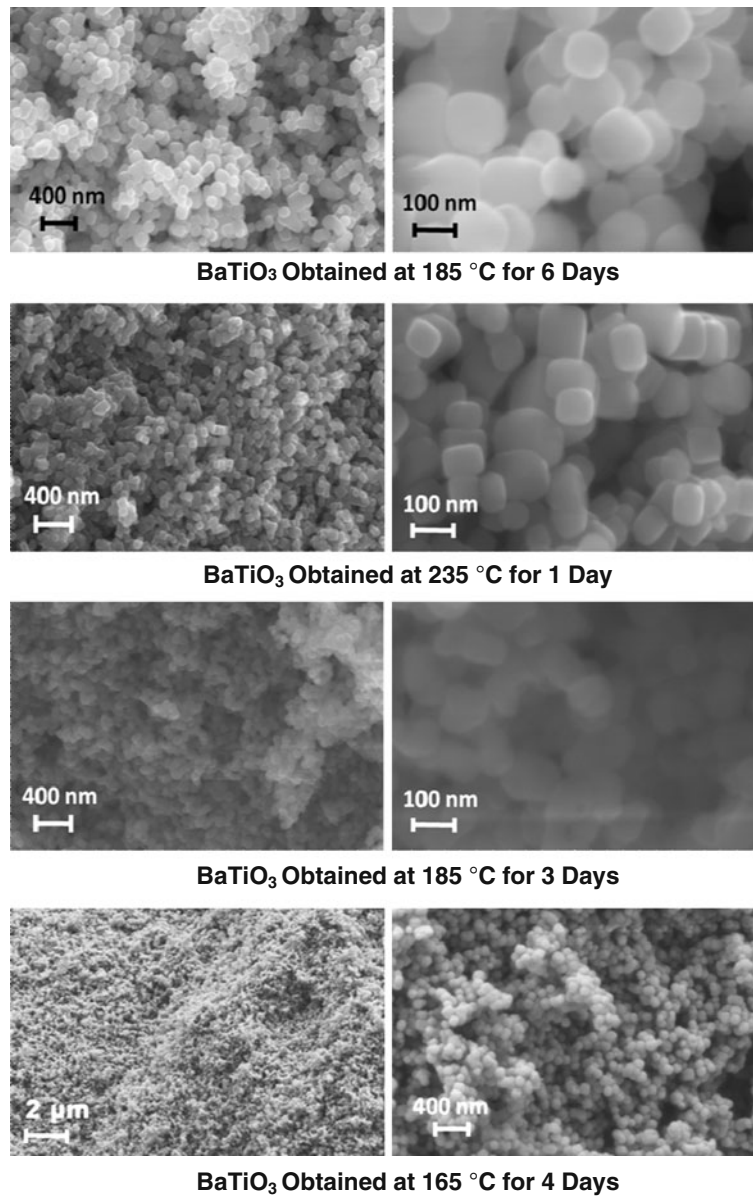


Figure 2. SEM micrographs of obtained BaTiO<sub>3</sub> powders.

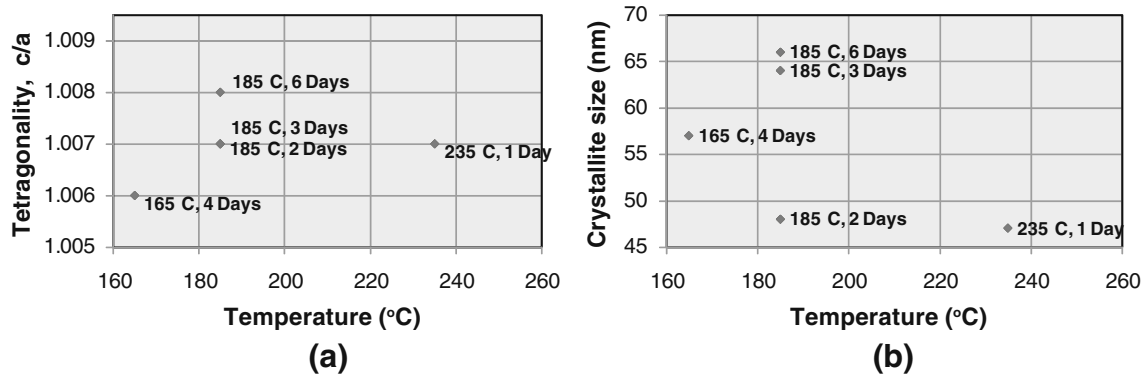


Figure 3. (a) Tetragonality, and (b) crystallite size (nm) for different processing temperatures and times of obtained BaTiO<sub>3</sub> nanopowders.

( $c/a \sim 1.008$ ) (figure 3). This is, to the best of our knowledge, the lowest reaction temperature with this high tetragonality reported in literature although the reaction time here is quite long i.e. 6 days.

It is generally believed that there is a decrease in tetragonal distortion with decreasing particle size below 1  $\mu\text{m}$ . Arlt *et al* (1985) reported that at grain sizes  $<0.7 \mu\text{m}$  the permittivity strongly decreases and the lattice gradually changes from tetragonal to pseudocubic. Uchino *et al* (1989) showed that the transformation from tetragonal to cubic symmetry occurred at a critical particle size of 0.12  $\mu\text{m}$ . Begg *et al* (1994), however, indicated that a hydrothermal BaTiO<sub>3</sub> powder with a particle size  $>0.27 \mu\text{m}$  was completely tetragonal and with a particle size  $<0.19 \mu\text{m}$  was a fully cubic phase. In this study largest  $c/a$  value of 1.008 is observed for crystallite size,  $\sim 66 \text{ nm}$  (figure 3). An increase in particle size is observed with increase in reaction time.

### 3.8 Transformation mechanism

The size and morphology of obtained product is quite different from the initial Ti-precursor (SEMs for TiO<sub>2</sub> are available elsewhere (Habib *et al* 2008)). This suggests that *in situ* transformation mechanism may not be crystallization mechanism for the formation of BaTiO<sub>3</sub> particles. Dissolution of TiO<sub>2</sub> into Ti(OH)<sub>x</sub><sup>4-x</sup> species must have occurred and precipitated BaTiO<sub>3</sub> nucleation by reaction with barium ions or complexes in solution, followed by recrystallization or growth i.e. dissolution–precipitation transformation mechanism. Barium titanate particles obtained by this route are usually different from the precursor titania particles with regard to their size and shape (Eckert *et al* 1996; Hu *et al* 2000).

## 4. Conclusions

Tetragonal BaTiO<sub>3</sub> ( $\sim 66 \text{ nm}$ ) nanopowders are synthesized via solvothermal route using an equal ratio of ethanol–water mixture. The  $c/a$  value of the BaTiO<sub>3</sub> powder samples prepared at 185°C increases with reaction time. The highest tetragonality ( $c/a = 1.00828$ ) is observed for samples reacted at 185°C for 6 days. The use of ethanol along with water as a solvent in 1:1 ratio proved to be beneficial in stabilization of tetragonal BaTiO<sub>3</sub>. The dissolution–precipitation appears to be a responsible transformation mechanism for the crystallization of BaTiO<sub>3</sub> from particulate TiO<sub>2</sub> precursor.

## References

- Arlt G 1987 *Ferroelectrics* **76** 451  
 Arlt G, Hennings D and de With G 1985 *J. Appl. Phys.* **58** 1619  
 AXS B 2005 *TOPAS V3: General profile and structure analysis software for powder diffraction data*, Karlsruhe  
 Begg B D, Vance E R and Nowotny J 1994 *J. Am. Ceram. Soc.* **77** 3186  
 Bell A J, Moulson A J and Cross L E 1984 *Ferroelectrics* **54** 487  
 Buessem W R, Cross L E and Goswami A K 1966 *J. Am. Ceram. Soc.* **49** 33  
 Chen D and Jiao X 2000 *J. Am. Ceram. Soc.* **83** 2637  
 Christensen A N 1970 *Acta Chem. Scand.* **24** 2447  
 Dinnebier R E and Billinge S J L 2008 *Powder diffraction—theory and practice* (Cambridge, UK: The Royal Society of Chemistry)  
 Dutta P K and Gregg J R 1992 *Chem. Mater.* **4** 843  
 Dutta P K, Asiaie R, Akbar S A and Zhug W 1994 *Chem. Mater.* **6** 1542  
 Eckert J O Jr, Hung-Houston C C, Gersten B L, Lencka M M and Riman R E 1996 *J. Am. Ceram. Soc.* **79** 2929  
 Habib A, Stelzer N and Haubner R 2008 *Mater. Sci. Eng.* **B152** 60  
 Habib A, Stelzer N and Haubner R 2009 *Solid State Phenom.* **151** 108  
 Hench L L and West J K 1990 *Principles of electronic ceramics* (New York: Wiley)  
 Hu M, Kurian V, Payzant E, Andrew R, Claudia J and Hunt R D 2000 *Powder Technol.* **110** 2  
 Kajiyoshi K, Ishizawa N and Yoshimura M 1991 *J. Am. Ceram. Soc.* **74** 369  
 Kanata T, Yoshikawa T and Kubota K 1987 *Solid State Commun.* **62** 765  
 Kiss K, Magder J, Vukasovich M S and Lockhart R J 1966 *J. Am. Ceram. Soc.* **49** 291  
 Kwon S-G, Park B-H, Choi K, Choi E-S, Namb S, Kimc J-W and Kimc J-H 2006 *J. Eur. Ceram. Soc.* **26** 1401  
 Lu S W, Lee B I, Wang Z L and Samuels W D 2000 *J. Cryst. Growth* **219** 269  
 Sun W, Li C, Li J and Liu W 2006 *Mater. Chem. Phys.* **97** 481  
 Uchino K, Sadanaga E and Hirose T 1989 *J. Am. Ceram. Soc.* **72** 1555  
 Vivekanandan R, Phillip S and Kutty T R N 1987 *Mater. Res. Bull.* **22** 99  
 Wu M, Xu R, Feng S H, Li L, Chen D and Luo Y 1996 *J. Mater. Sci.* **36** 6201  
 Wu M, Junbiao L, Wang G, Huang A and Luo Y 1999 *J. Am. Ceram. Soc.* **82** 3254  
 Xu H and Gao L 2003 *J. Am. Ceram. Soc.* **86** 203  
 Yoon D-H 2006 *J. Ceram. Process. Res.* **7** 343  
 Young R A 1993 *The Rietveld method* (New York: Oxford University Press Inc.)  
 Zhang M S, Yin Z, Chen Q, Zhang W and Chen W 2001 *Solid State Commun.* **119** 659